Dynamics and Vibration of a Single Axis Active Magnetic Bearing System for Small-sized Rotating Machinery

Ichiju SATOH, Yuji SHIRAO

Ebara Research Co.,Ltd
2-1,Hon fujisawa 4-chome,Fujisawa-shi,251 Japan
tel:+81-466-83-7666; fax:+81-466-82-9371; e-mail:satoh07018@erc.ebara.co.jp

Yoichi KANEMITSU

Dept. of Intelligent Mechanical Eng., Kyushu University
6-10-1,Hakozaki, Higashi-ku, Fukuoka-shi, 812-81 Japan

Abstract: We have been studying a single axis active magnetic bearing for small-sized and high speed rotating machinery as a trial. The trial model has very simple structure and is very small in size and light in weight. The model is composed of two passive radial magnetic bearings utilizing repulsion force of permanent magnets and one active magnetic bearing in axial direction. Experimental results show that an unstable vibration occurs when the rotor was driven over 15,000rpm. In this paper, we discuss the cause and mechanism of this vibration. On the basis of computer analysis using the model with gyroscopic effect, it is clarified that coincidence of the node for conical mode and the damper cause the unstable vibration. Finally, we discuss countermeasures of this vibration.

1. Introduction

Five-axis active type magnetic bearings are widely used by general industries for supporting their rotating machinery. However, as five-axis active type magnetic bearings comprise five electromagnets and control circuits, it becomes difficult to meet current machinery requirements, such as compactness, lightweight and energy-saving features. One way to achieve such requirements would be to reduce the control axes by combined use of a passive magnetic bearing equipped with permanent magnets.

There have been very few practicalized passive magnetic bearings until recently. This is because passive magnetic bearings, which make use of either repulsion or attraction forces, feature less stiffness and smaller damping effect than those of active types. In particular, the passive axis has almost no damping force, thus necessitating a supplementary eddy-current damper or some other kind of mechanical damper.

However, recent development of stronger permanent magnets, better damping materials, and progress in magnetic field analysis are making it easier for the practicalization of passive magnetic bearings. Consequently, researches on passive magnetic bearing system which use permanent magnets are increasing[1], [2]. However, in those refered papers which describe single axis active magnetic bearing, vibration problem in passive magnetic bearing systems is not sufficiently discussed.

The authors are currently carrying out research and development on a single-axis active magnetic bearing system, featuring passive stabilization of the four degrees of freedom in the radial direction by the repulsive force of permanent magnets. The configuration of a prototype system, developed by the authors, is extremely simple. One problem encountered during the rotating test using the prototype system was an occurrence of a self-excited vibration in the conical forward whirling, when the rotation speed reached approximately 15,000[rpm].

The following outlines the configuration of the present single-axis active magnetic bearing prototype system, and clarifies the cause of the above vibration by rotational test and analytical results, and discusses means of coping with this vibration.

2. Single-axis Magnetic Bearing System

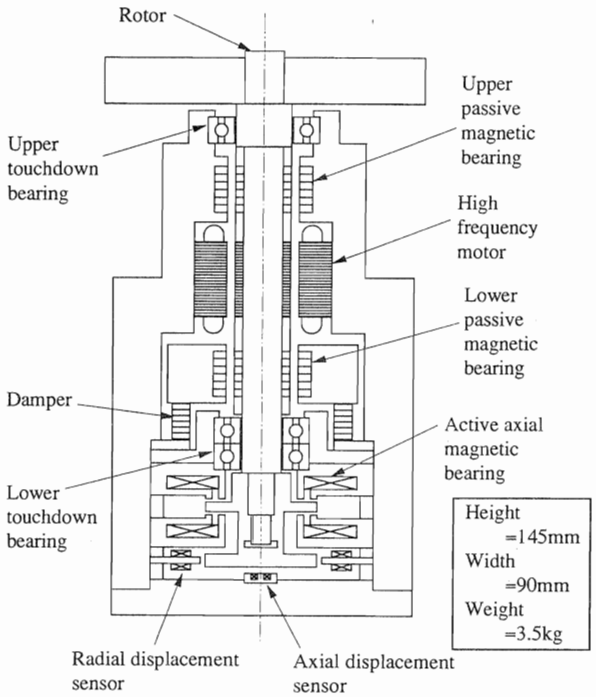

Fig.1 A single axis active magnetic bearing system

Figure 1 shows the schematic diagram of the single-axis magnetic bearing prototype system. A high frequency motor is in the center and two permanent magnet repulsive type radial bearings, with identical configurations, are above and below it. The center of gravity of the rotor is at approximately the center of the upper repulsive radial bearing. A laminated-rubber-type damper is used for the lower repulsive bearing section, with the repulsion magnet section being elastic supported by the stator via the damping material. An axial control magnetic bearing is situated at the lower end of the rotor.

2.1 Passive Radial Bearing

The simply structured repulsive type radial bearings was selected for the present prototype system, consequent to emphasis put on easy assembly and disassembly. In permanent magnet repulsive type radial bearings, stable stiffness can always be obtained along the radial direction, while only unstable stiffness occurs along the axial direction.

2.1.1 Configuration

The permanent magnet repulsive type radial bearing used for the present system constituted stacks of ring-shaped permanent magnets, magnetizing along the axial direction, in a way that the homopolarity of both the rotor and stator sides faced each other. Identically configured magnets were above and below the motor. Nd-Fe-B magnets, which feature the maximum energy product available currently, were used.

2.1.2 Static and Dynamics characteristics

The stable radial stiffness $K_r = 60.7$[N/mm] and the unstable axial stiffness $K_z = -178.7$[N/mm] was obtained by linear approximation of measurements. The unstable stiffness is three times as large as the stable stiffness. As both the upper and lower radial repulsive bearings are identically configured, measurement was made only on one radial bearing.

Figure 2 shows the frequency response of radial displacement of the rotor versus the exciting force applied by an impulse hammer in the radial direction. The radial bearing is not equipped with a damper and the rotor is suspended by magnetic bearings. The peak at the proximity of 60[Hz] is the natural frequency of the conical motion, while that at the proximity of 125[Hz] is the same of the parallel motion. Both natural frequencies exhibit sharp peaks and it proves that there was almost no damping of the permanent magnet repulsive force.

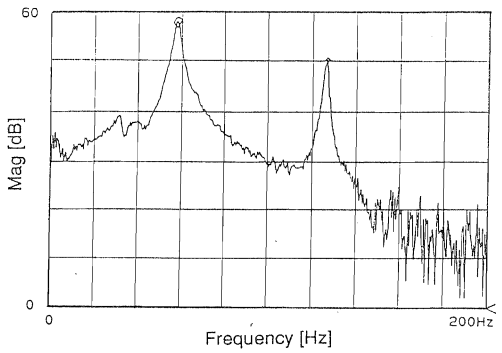

Fig. 2 Frequency response of the system without damper

2.2 Damper system

In case we drive the rotor over critical speeds, it becomes necessary to implement a damper which will effectively work for the conical and parallel vibrations.

2.2.1 Configuration

Figure 3 shows a schematic diagram of the damper system for radial vibration. The laminated-rubber-type damper is composed of rubber sheets and thin stainless steel plates piled up alternately. The damper can support the lower radial bearing stator (magnet holder) tightly in axial direction against to its negative stiffness, although supported flexibly in radial direction. The flexible support and elastic hysteresis of material can realize suppression of the rotor vibration which is transmitted to the stator by the repulsive force of the magnetic bearing. Consequently, a reduction in the radial vibration is achieved.

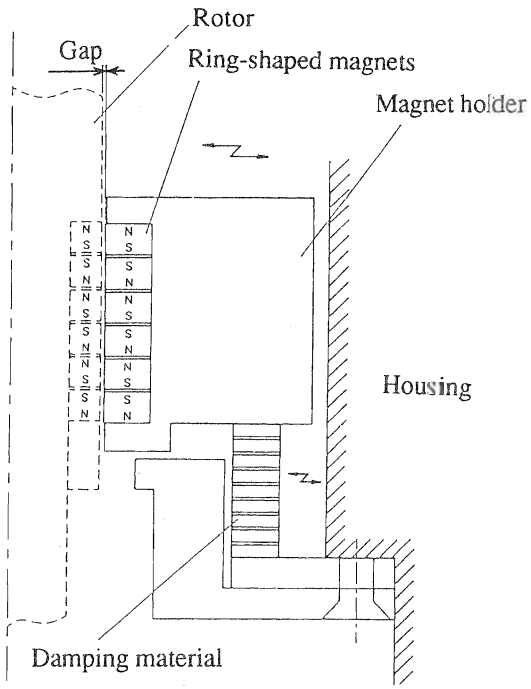

Fig. 3 Damper system

2.2.2 Damper property

The impulsive response of the damper system was studied by measuring the displacement resulting from impact excitation, by an impulse hammer, on the magnet holder. The holder was attached on a damper which was secured on a base, i.e. the damper with holder was not installed in the system. Figure 4 shows diagrams with the measured transfer functions. These diagrams indicate that the damper system can be expressed as a vibration system with one degree of freedom as Eq. (1) . As the damping effect by the present damper was extremely favorable, there was damped peak at the resonance frequency.

$$G(s) = \frac{X(s)}{F(s)} = \frac{1}{ms^2 + cs + k} \tag{1}$$

wherein, the mass is indicated as m; the damping coefficient and spring constant as c and k respectively.

The damping coefficient c is determined by the material property of the rubber. On the other hand, to obtain the sufficient damping

effect, the mass m and the spring constant k should be selected in the region where the following equation is satisfied.

$$f_{co} \leq \frac{1}{2\pi}\sqrt{\frac{k}{m}} \leq f_{pa} \qquad (2)$$

wherein, the natural frequency of the conical mode and the parallel mode are indicated as f_{co} and f_{pa} respectively. However, the natural frequency of the prototype damper was f_{nd}=170[Hz] , which is rather high value compare to designed frequency.

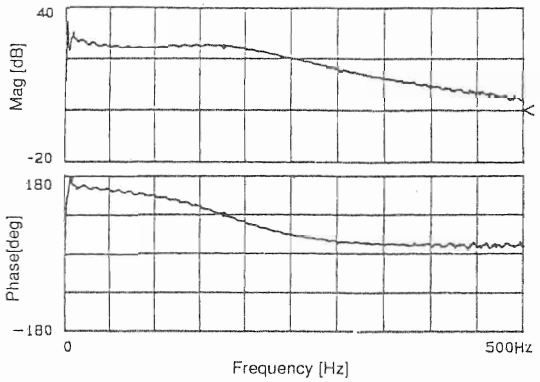

Fig. 4 Frequency response of damper system

2.3 Rotor-bearing system

Figure 5 shows the frequency response of the system measured by the method mentioned previously. The lower radial bearing is equipped with the prototype damper and the rotor is in a suspended state.

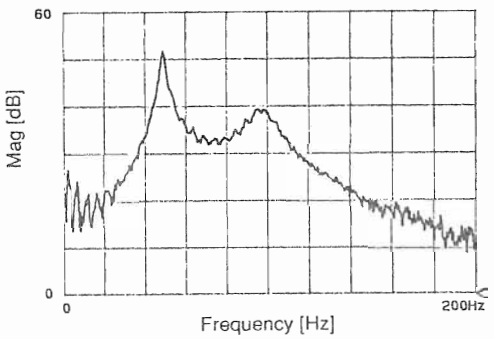

Fig. 5 Frequency response of the system with damper (Experiment)

Compared to the case where no damper was used (see Fig. 2) , use of the damper resulted in both peaks frequency being lower (f_{co}≈50[Hz] and f_{pa}≈100[Hz]) . Although, the peak of parallel mode (right peak) is damped well, the damping of conical mode (left peak) is not sufficient because the eigen-frequency of the damper does not lie in the region of Eq. (2).

3. Results of rotation test

Figure 6 shows a time history diagram of a rotation test. The abscissa represents the elapse time, the topmost curve represents the rotation speed, and the second and third waveforms represent the vibration of the rotor in the x and y directions respectively. A conical mode resonance is indicated at approximately 3,000 [rpm], with an increase in amplitude. A parallel mode resonance frequency is indicated at approximately 6,000 [rpm], but the amplitude is kept small by the damping effect of the damper. With the amplitude maintained small, a rotation speed of approximately 15,000[rpm] is reached. From this point on, however, there is a rapid increase in the vibration amplitude, the outcome of which the rotor makes contact with the touchdown bearing.

Figure 7 shows results of frequency analysis by FFT analyzer on this vibration. It is shown that the 62.5[Hz] conical vibration component appears greater than the 252.5[Hz] rotation component. This data is according to measurements made just the rotor made slightly contact with the touchdown bearing, therefore, harmonic vibrations of 62.5[Hz] had appeared.

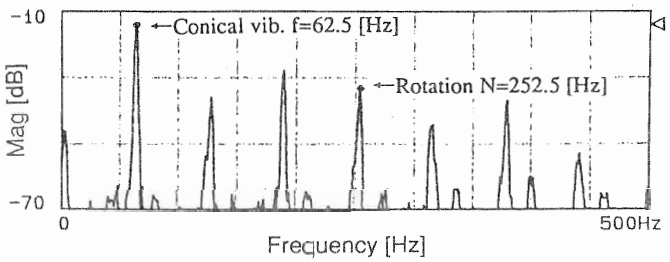

Fig. 7 Result of a frequency analysis of the vibration

4. Analysis on the Cause of the Conical Vibration

An analytical model was made, with consideration given on the gyroscopic effect, to study the cause and mechanism of, as well as measures against the said conical vibration. Take note that

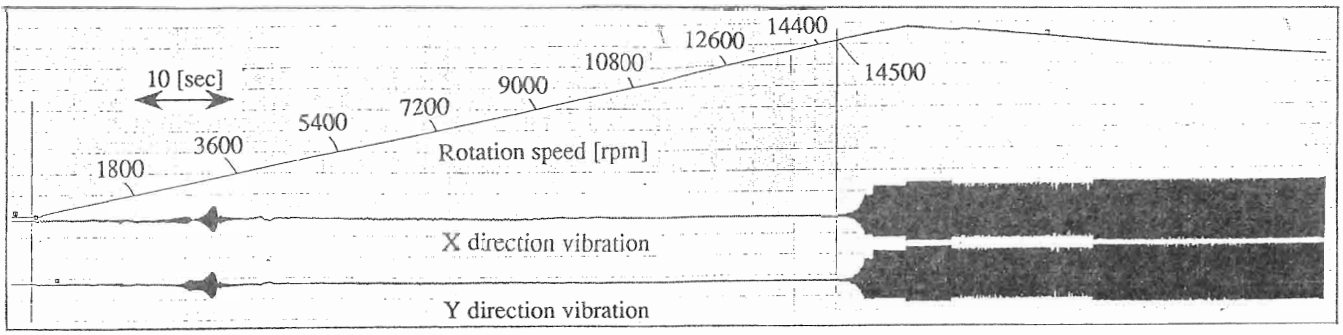

Fig.6 Time history of the conical vibration (Experiment)

the analysis done here is based on the rigid mode, with no consideration given on the flexible mode of the rotor.

4.1 Analytical model

Figure 8 shows the dynamic model of the system. The mass of the rotating body and the moments of inertia are indicated as M, I_p and I_d, respectively. The radial stiffness of the repulsive bearing is indicated as K_r, isotropic in the x and y directions. The center of gravity G is indicated as L_1 from the upper bearing and L_2 from the lower bearing.

Considering a motion of rigid body where the origin of x-y coordinate is the rotating body center of gravity G at the steady suspended position, the center of gravity G position is indicated as x_g and y_g, and the small-inclination angles of the rotation center axis, around the x- and y-axes, indicated as θ_x and θ_y,

$$\begin{cases} x_1 = x_g + L_1\theta_y \quad , \quad y_1 = y_g - L_1\theta_x \\ x_2 = x_g - L_2\theta_y \quad , \quad y_2 = y_g + L_2\theta_x \end{cases} \tag{3}$$

considering the axial symmetry in structural terms, and using the complex variable

$$\begin{cases} r_g = x_g + \mathrm{j}\, y_g \\ r_3 = x_3 + \mathrm{j}\, y_3 \\ \theta = \theta_x + \mathrm{j}\theta_y \end{cases} \qquad \left(\mathrm{j} = \sqrt{-1}\right) \tag{4}$$

the following equation of motion, in which consideration is given on the gyroscopic effects, can be used:

$$\begin{cases} M\ddot{r}_g + K_r r_g = \mathrm{j}K_r\left(L_1 - L_2\right)\theta - K_r r_3 \\ I_d\ddot{\theta} - \mathrm{j}I_p\omega\dot{\theta} + K_r\left(L_1{}^2 + L_2{}^2\right)\theta = -\mathrm{j}K_r\left(L_1 - L_2\right)r_g - \mathrm{j}K_r L_2 r_3 \\ m\ddot{r}_3 + c\dot{r}_3 + \left(K_r + k\right)r_3 = K_r r_g + \mathrm{j}K_r L_2\theta \end{cases} \tag{5}$$

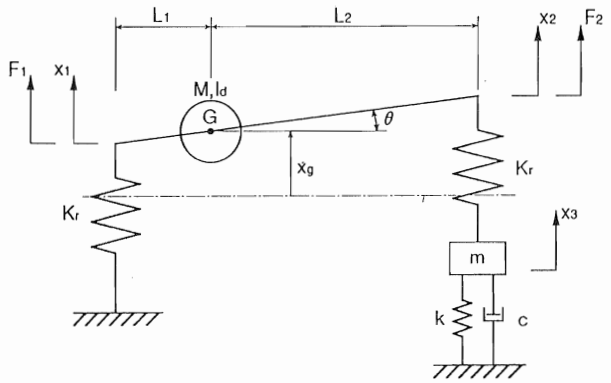

Fig. 8 Analytical model

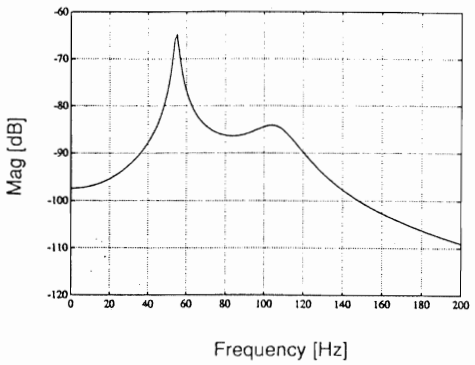

Fig. 9 Frequency response of the rotor with damper

Figure 9 shows the calculated frequency response of radial displacement of the rotor versus the excitation force of the rotor, using the dynamic model mentioned above. The validity of this model is assured by the fact that the characteristics are almost identical to those of the test results shown in Fig. 5.

4.2 Cause of the conical vibration

Figure 10 shows calculation results on natural frequency f_n versus rotation speed N of each mode. The resonance frequency for the conical modes is at approximately 60 [Hz], that for the parallel modes is at approximately 110 [Hz], values that match well with those of test results. The circle symbols in Fig. 10 represent actually measured values of cases where the casing was impact-excited during rotation. This measurement was only possible in the conical modes, wherein the damping was minimal, and the results match well with calculation results.

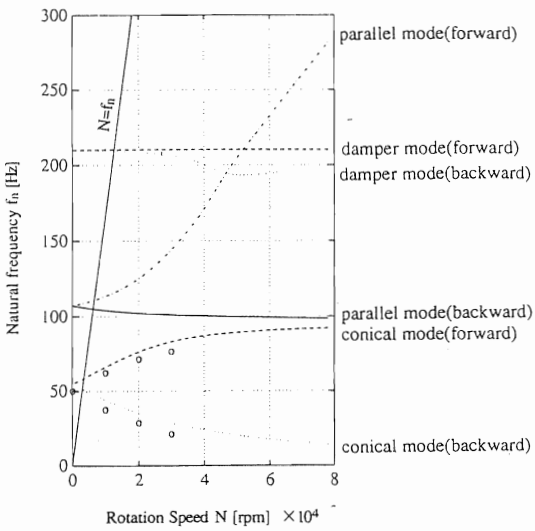

Fig. 10 Natural frequency map

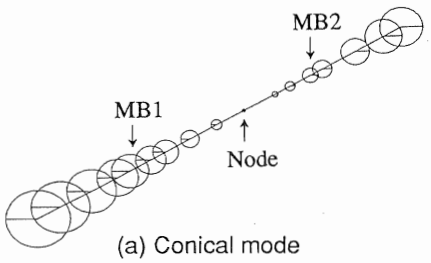

(a) Conical mode

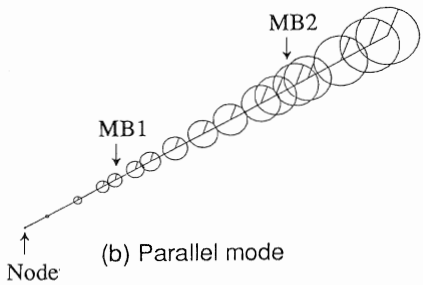

(b) Parallel mode

Fig. 11 Mode shape of natural vibrations

Figure 11 shows the mode shape at resonance frequencies of both the conical and parallel modes. Both modes deviate from "pure" conical and parallel one, because the center of gravity is not located in the center of two bearings.

Figure 12 shows the root loci on eigenvalue changes in each mode versus the rotation speed. Figure 12 (a) shows those in all modes, i.e. the conical, parallel, and damper modes. Each mode, situated initially at positions indicated by the circle symbols when the rotation speed was at zero, became divided into two modes, i.e. forward and backward, with an increase in the rotation speed. Although the damping of the conical mode is overall smaller, the eigenvalue of the forward mode is seen to undergo changes at a particular region, seeming to graze off an imaginary axis. It means that the damping of conical forward mode becomes zero at a certain rotation speed.

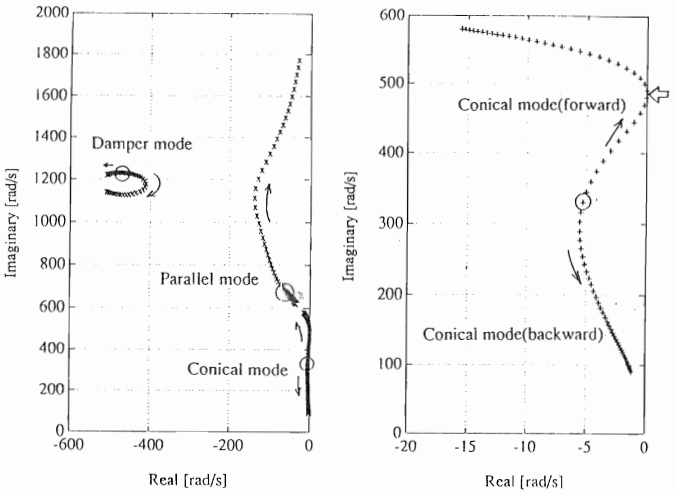

(a) All modes (b) Conical modes

Fig. 12 Root loci

Figure 13 shows changes in the damping ratio of natural vibrations versus the rotation speed. It is clearly indicated in the diagram that the damping ratio of the forward conical mode becomes almost zero in the region covering approximately 15,000 -20,000[rpm]. Note that the calculation was made here under the conditions that the damping ratio of the original plant was equal to zero and that of damper was 0.5. Studying the above, it was found that as for this system, the node position of the forward conical mode underwent significant changes along changes in the rotation speed.

Figure 14(a)- (c) show changes in the forward conical mode nodes at rotation speed ω=12,000, 19,200, and 24,000[rpm] schematically. The node at ω=12,000[rpm] is at a position which is three-quarters between the bearings, while a conical mode node moves to the position in the center of the lower bearing at ω=19,200 [rpm]. As a damper was used for the lower bearing of the present prototype system, the rotor vibration could not be transmitted to the damper for such mode configuration. Consequently, a conical vibration in the forward direction becomes generated in the proximity of 20,000[rpm]. As acknowledged from the diagram for the case of ω=24,000[rpm], the node continues shifting along the increasing in the rotation speed and a situation is reached where a damping by damper works again.

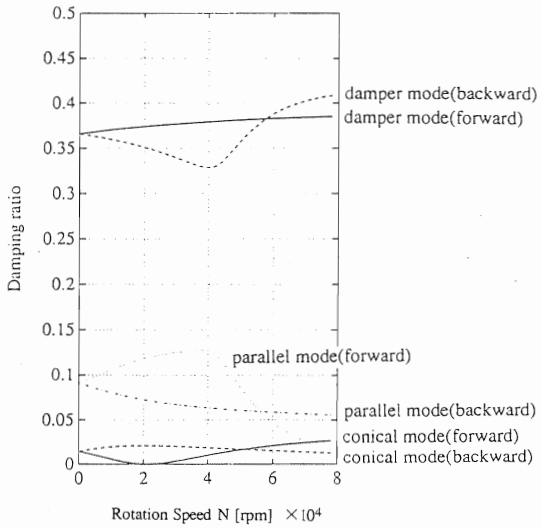

Fig. 13 Damping ration of natural vibrations

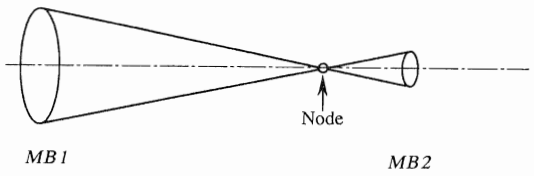

(a) Rotation speed is 12,000rpm

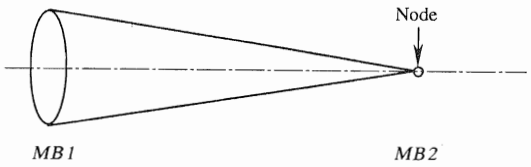

(b) Rotation speed is 19,200rpm

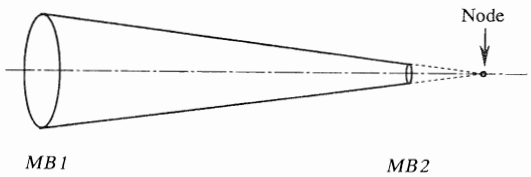

(c) Rotation speed is 24,000rpm

Fig. 14 Changing of conical forward mode's node

5. Improvement

5.1 Countermeasure

The cause of the said unstable vibration occurrence was found to be due to the coincidence between the forward conical mode node, which shifted along the increase in the rotation speed, and the damper section at a given rotation speed. And, shifting of

the node is resulting from the coupling of the conical and parallel motion, which is obvious from Eq. (5) by a term (L_1-L_2). Therefore, to set L_1=L_2, which means the center of gravity is located just in the center of upper and lower bearings, the coupling is canceled and these two modes become "pure" conical and parallel motion. However, as for measures against this vibration, consideration was made to keep overall configurational changes at a minimum. Consequently, the most simple countermeasure which was concluded would be to equip the upper magnetic bearing with a damper as well. It is forecasted that the damping effect would be maximized by doing so, as the conical vibration was such that caused the lower bearing to become a node, resulting in an increase in the amplitude of the upper bearing.

5.2 Analysis results using two dampers

A model was made wherein identical dampers were used for both the upper and lower bearings, and eigenvalue analyses were carried out in the same way as discussed previously. Figure 15 shows calculated changes in the damping ratio of natural frequencies versus the rotation speed. An extra mode is resulting from the addition of another damper. There was no case where the forward conical mode damping was zero and an improvement in the damping ratio of each modes are indicated.

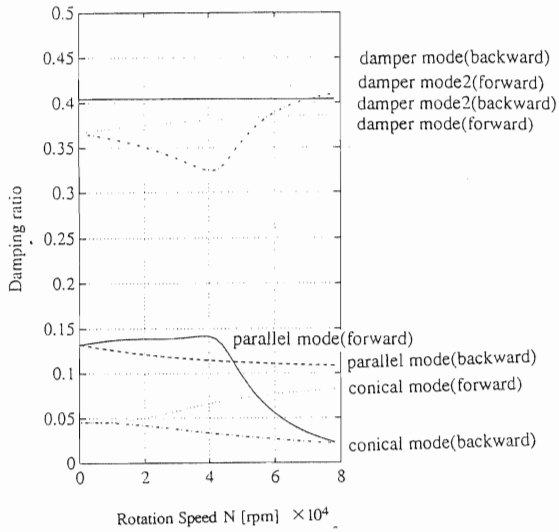

Fig. 15 Damping ration of eigenvalues for the case two dampers were used

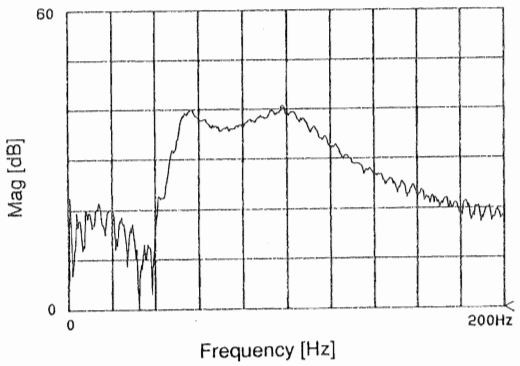

Fig. 16 Frequency response of the system with two dampers

5.3 Experimental results using two dampers

Experiments were carried out, with identical dampers equipped on both the upper and lower bearings. Figure 16 shows the frequency response of the system measured by the method mentioned previously. Compared to the case where one damper was used (see Fig. 5), use of two dampers resulted in both peaks are damped sufficiently.

Figure 17 shows the rotation test results. The ordinate represents the vibration amplitude and the abscissa represents the rotation speed. Although the amplitude increased at the conical mode resonance speed at 3,000[rpm], it decreased to below 10[μ m] along the increase in the rotation speed, and a stable rotation was achieved up to 75,000[rpm].

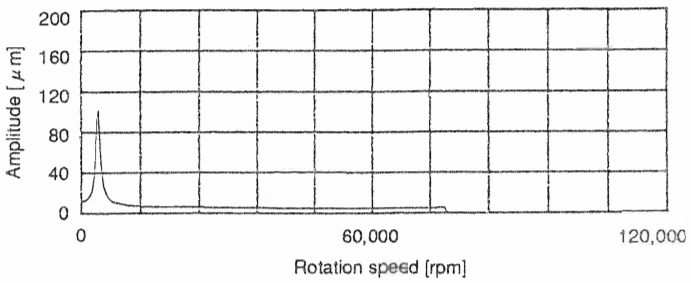

Fig. 17 Result of high speed rotational test

6. Conclusions

A prototype single-axis active magnetic bearing system, featuring the laminated-rubber-type damper, was developed to fulfill the demand for a compact, lightweight, and energy-saving magnetic bearing system.

As the initial rotation test indicated an unstable forward conical mode, numerical analysis was carried out using a model with consideration given on the gyroscopic effect. The cause of the unstable forward conical whirling motion was traced down to the shift of this mode's node to the damper. Consequently, configurational changes were made on the actual prototype system and high speed stable rotation of up to 75,000[rpm] was achieved.

Although passive magnetic bearings have many problems such as demagnetization of permanent magnets, heating expansion and deterioration of damping materials, the authors intend to continue this research for making it possible to apply this bearing system for pumps and other rotating machinery.

References

[1] J.K.Fremery,"Radial Shear Force Permanent Magnet Bearing System with Zero-Power Axial Control and Passive Radial Damping " , Proc. of 1st Int. Sympo. on Magnetic Bearings , Zurich, pp.25-31 , 1988

[2]M.Miki, et al. ,"Single Axis Active Magnetic Bearing System with Mechanical Dampers for High Speed Rotor ",Proc. of 2nd Int. Sympo. on Magnetic Bearings ,Tokyo, pp.183-187,1990